Local wave grouping in a parameter-gradient system and its formation mechanism

Huimin Liao,[1] Yangle Wu,[1] Jianglei Yu,[1] and Qi Ouyang[1,2,3,*]
[1]*School of Physics, Peking University,*
[2]*The Beijing-Hong Kong-Singapore Joint Center for Nonlinear and Complex System (PKU),*
[3]*Center for Theoretical Biology, Beijing 100871, China*
(Received 6 September 2007; published 25 January 2008)

In a ferroin-catalyzed Belousov-Zhabotinsky (BZ) reaction-diffusion system with reagent concentration gradients, we observed in the experiment a type of spirals with local waves forming groups. Here, we propose an interpretation of the wave grouping phenomenon. The wave grouping mechanism can be well explained in terms of the cooperation of the excitability gradient and the Doppler effect induced by spiral tip's meandering. In the simulation based on three-dimensional reaction-diffusion system using Oregonator model, spiral patterns analogous to the experiment observation are well reproduced when the parameter gradient in the z direction is introduced.

DOI: 10.1103/PhysRevE.77.016206 PACS number(s): 82.40.Bj, 82.40.Ck, 47.54.−r, 47.20.Ky

I. INTRODUCTION

Pattern formation has been studied in many experimental systems [1]. Early experiments include chemical [2–4], biological [5], fluid systems [1,6], which are well designed to meet certain pattern formation conditions. For chemical reactions, to keep the system far from equilibrium, refresh of the reagents is necessary. The spatial open reactor designed first in Swinney's group [7], has been widely used to systematically study pattern formation in reaction-diffusion systems. Though the pattern formation in such an system is complex, some simple and effective explanations have been achieved, such as the one-dimensional (1D) or 2D mechanisms on Doppler instability [8] and long-wavelength instability [9] of spiral waves.

In our recent experiment on spirals in a ferroin-catalyzed BZ reaction-diffusion in a spatial open reactor, we found a type of meandering spiral, which demonstrated local wave grouping, i.e., local dense waves group in twos, and sparse waves hold equal spacings [10]. To understand the unusual wave interaction in this phenomenon, we gave our first tentative explanation based on a hypothesis about the system's reaction dynamics. It assumed that the unusual wave interaction is caused by oscillatory dispersion, and omitted the influence on the wave propagation in the thickness direction. Our simulation results showed that in the cooperation of the Doppler effect and the oscillatory dispersion relation, local wave grouping could happen [10]. However, for the Oregonator model that we used to simulate the BZ reaction, a system with an oscillatory dispersion relation is rarely found to support meandering spiral, which is necessary to induce the Doppler effect. Thus we suspect that the wave interaction might not be 2D, but a 3D one. Some 3D mechanisms might induce spiral meandering and complex wave interaction simultaneously. In this paper, we discuss this character of the spiral waves, and give an explanation in terms of 3D wave interaction.

II. EXPERIMENT

We conduct our experiments in the ferroin-catalyzed BZ reaction in an open spatial reactor, as described in Ref. [11]. A thin porous glass disk, 0.4-mm thick and 25.4 mm in diameter (Vycor glass 7930, Corning), is served as the reaction-diffusion medium. Two continuously fed stirred reservoirs sandwich the glass disk; in each reservoir the reactants are maintained homogenous by a permanent feeding of fresh reactants. In our arrangement, the catalyst ferroin and malonic acid (MA) are separated in different reservoirs. In the following, we label the reservoir containing MA as reservoir A, and the other as reservoir B. Thus the catalyst concentration in the glass increases in going from reservoir A to reservoir B, while the MA concentration decreases in going from reservoir A to reservoir B. Thus strictly speaking, the pattern formed in the media should have 3D structures, and the images observed on the media surface are just the plan views of the oblique 3D structures [12]. The measurement in the experiments is a series of snapshot pictures taken by a CCD camera. The gray level of image corresponds to the light transmission in 3D chemical patterns in the glass disk through the z direction, which is positively correlated with the quantity of the oxidized catalyst ferriin. So that the image we observe is a projection of the patterns in the x-y plane.

In such an experimental system, without any external force meandering spirals spontaneously appear in a large range of parameters. A common meandering spiral is shown in Fig. 1(a), whose wavelength varies gradually in space because of the Doppler effect induced by the movement of the spiral tip, and the gradual variation of wavelength can construct a spiral-like superstructure [13]. Under certain conditions, dense waves with small spacing may form fine structures, with every two or three waves coming into group, the wave spacings change alternatively in space. An example of such a pattern is shown in Fig. 1(b). Commonly, if the spiral is meandering, the grouping occurs in the direction it drifts to, and in the opposite direction the waves are almost identical. But there are still some cases where wave grouping occurs in all directions. This happens when the spiral wavelength is small, and the spiral tip meanders just slightly or

*qi@pku.edu.cn

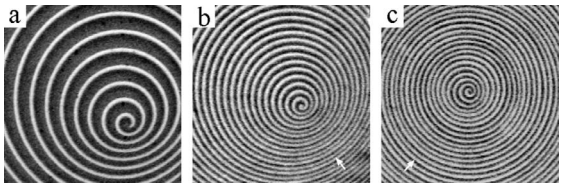

FIG. 1. Spiral waves with different fine structures. (a) A meandering spiral. $[MA]_0^A=0.6$ M, $[H_2SO_4]_0^B=0.4$ M, and $[NaBrO_3]_0^B=0.2$ M. (b) A meandering spiral with wave grouping. $[MA]_0^A=1.2$ M, $[H_2SO_4]_0^B=0.6$ M, and $[NaBrO_3]_0^B=0.23$ M. (c) A simple spiral with slightly wave grouping. $[MA]_0^A=1.2$ M, $[H_2SO_4]_0^B=0.8$ M, and $[NaBrO_3]_0^B=0.2$ M. Other reactants are the same: $[KBr]_0^A=0.03$ M, $[NaBrO_3]_0^A=0.2$ M, $[ferroin]_0^B=1.0$ mM. Each image is 11.3×11.3 mm^2. White arrows point out the wave grouping.

almost does not meanders. Figure 1(c) gives an example of such a case.

Series of experiments are conducted to explore the influence of some reagent concentrations on the spiral behavior. In each series of experiment, $[MA]_0^A$ is varied while $[H_2SO_4]_0^B$ is kept fixed. Then we change $[H_2SO_4]_0^B$ and repeat the experiments. The other conditions are kept fixed in all experiments. When $[H_2SO_4]_0^B$ is low, spiral wavelength is large and wave speed is slow. Spiral tips will always meander in these cases, but the waves will not group. When $[H_2SO_4]_0^B$ is high, spiral wavelength becomes small and wave speed becomes fast. Spiral tips tend to simply rotate in a small cycle; the waves will neither group under these conditions. Only when $[H_2SO_4]_0^B$ is at middle level, the waves may group with high enough $[MA]_0^A$, and the grouping become more obvious with the increase of $[MA]_0^A$. The influence of $[NaBrO_3]_0^B$ on the grouping is analogous to that of $[H_2SO_4]_0^B$. The grouping will not occur when $[NaBrO_3]_0^B$ is high or low; it can only occur at a small range of $[NaBrO_3]_0^B$ at middle level. The transition from wave grouping to no grouping (or vice versa) is gradual as a function of $[H_2SO_4]_0^B$ or $[NaBrO_3]_0^B$, accompanied with the change of the spiral's properties, such as the wavelength, the wave speed and the rotation style.

To get more information on the wave grouping phenomena, we carefully monitor the state of the spiral tip. Fig. 2(a) and 2(b) present two snapshots corresponding, respectively, to the same phase of the tip rotation in two adjacent periods.

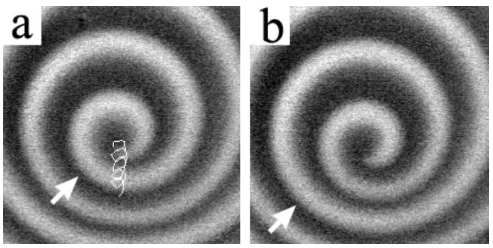

FIG. 2. Snapshots of the state of spiral tip in two adjacent periods. (a) $t=0$. (b) $t=7$ s. The flowerlike white line in (a) shows the trajectory of the tip. The experimental condition is the same as in Fig. 1(b). Each image is 1.9×1.9 mm^2.

One observes that at the moment of Fig. 2(a), the first downwards wave following the tip is relatively thin, and the second one [labeled by the arrow in Fig. 2(a)] is thicker. After one period of spiral rotation [Fig. 2(b)], the newly emitted first downwards wave becomes thick, and the second and the third one, i.e., the first and the second one a period before still keeps thin or thick [labeled by the arrow in Fig. 2(b)]. In contrast, the upwards waves all develop into thick ones immediately after emitted, with no obvious differences in thickness. Thus, the wave grouping should be originated from the spiral tip.

III. SIMULATION

We use two-variable Oregonator model to simulate the corresponding reaction-diffusion system. Considering that there are reagent concentration gradients in the system, the important control parameters are the concentrations of $NaBrO_3$ and MA, which are reserved in the model [14]:

$$\frac{\partial u}{\partial t}=\frac{1}{\varepsilon}\left[u(A-u)+fBv\frac{qA-u}{qA+u}\right]+D_u\nabla^2u,$$

$$\frac{\partial v}{\partial t}=Au-Bv+D_v\nabla^2v. \tag{1}$$

The variables u and v in Eq. (1) represent the concentration of $HBrO_2$ and that of oxidized catalyst ferriin, respectively; A and B represent $[NaBrO_3]$ and [MA], respectively; ε and q are constants determined by the reaction rate constants, and f is a stoichiometric coefficient. According to Ref. [15], we set $\varepsilon=0.01$, and $q=2\times10^{-4}$. The value of f is related to A and B. Since the dependence of f on A and B is still not very clear, we leave f as an independent variable. D_u and D_v are diffusion coefficients of u and v variables, respectively. With choosing a time unit (TU)=1 s, and a spatial unit (SU) =0.29 cm, and considering the difference of the molecular weights of $HBrO_2$ and ferriin [16], we set $D_u=5\times10^{-5}$ SU^2/TU [17] and $D_v=3\times10^{-5}$ SU^2/TU.

A $400\times400\times30$ or $800\times800\times30$ grids simulation area is used with no-flux boundary. The Laplacian is calculated with 19-point approximation [18]. Spatial step h is 0.01 SU; time step dt is 0.01 TU. To simulate the real concentration gradients, parameters are kept invariant in the x and y direction, while A, B, f vary linearly in the z direction. In the following, we use A_l, B_l, f_l to represent parameters of the lowermost layer, and A_u, B_u, f_u to represent those of the uppermost layer.

In such a 3D system with parameter gradients, many kinds of 3D spiral conformation can be observed. With some parameters, meandering spirals with wave grouping will emerge. A typical example of such a pattern is shown in Fig. 3. It demonstrates the projection of v variable (superposition of v in all layers) in the x-y plane, reminiscent of the image observed in experiment. The pattern in Fig. 3 bears many similarities with the experimental result of Fig. 1(b). In the drifting direction of the spiral tip (from low-right to up-left), the waves are compressed and group in twos. The two waves in the same group are different in shape: one wave is thin,

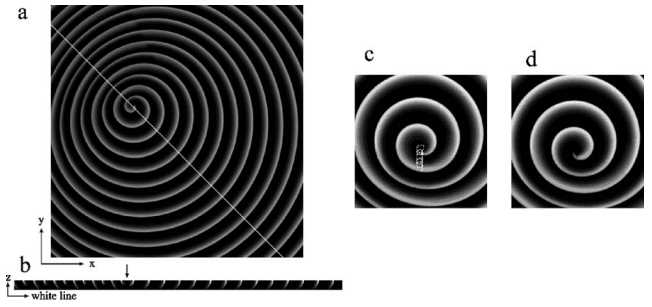

FIG. 3. Patterns simulated with the Oregonator model of Eq. (1). (a) Distribution of superposition of v variable of all layers in the x-y plane. The area size is 8.00×8.00 SU^2. (b) The section plane along the white line in (a). The area size is 10.40×0.30 SU^2. (c), (d) snapshots of the state of spiral tip in two adjacent periods [the drift direction of spiral tip is different from that of (a)]. The flowerlike white line in (c) shows the trajectory of the tip. The area size is 2.40×2.40 SU^2. Parameters are A_l=0.038, B_l=0.32, f_l=3.50, A_u=0.060, B_u=0.50, f_u=3.00.

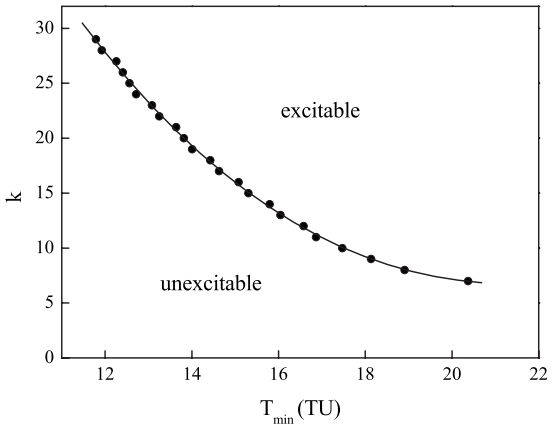

FIG. 4. The minimal period $T_{\min}$ of 1D wave train under the local parameter condition of layer k (numbered from bottom to top). Parameters are the same as in Fig. 3.

and another is thick. While in the opposite direction the waves travel in an equally spaced sequence, all identical in shape. The wave grouping in the left upward direction emerges from near the tip, as in the experiment [Figs. 3(c) and 3(d)].

To reveal the underlying formation mechanism of the wave grouping, we also monitor the waves in the section plane. Figure 3(b) present a special section plane that across the spiral tip along the white line in Fig. 3(a). The gray level in the figure is proportional to the v variable. One observes that crescent-shaped waves are generated from the spiral "tip" (labeled by arrow) and propagate outwards. The shape of the waves is very similar to pinwheel waves that were observed in the earlier experimental reports [19–22]. On the left side of the tip, waves are dense and their tails become shorter for every other waves. We thus observe an alternation of long-tail and short-tail waves. On the right side, waves are sparse and their tails all can touch the bottom. Obviously, in this case the difference in the shape of crescent waves causes the difference in the z projection of waves present in Fig. 3(a).

The shortening of some wave tails in the dense waves can be understood by considering the excitability of the media in the z direction. In our simulation, every layer along z direction has a different excitability. Figure 4 gives the lowest period $T_{\min}$ of 1D waves calculated under the local parameter condition of every layer. The excitability of the system is reversely related to $T_{\min}$; a smaller $T_{\min}$ means a larger excitability of the system, because when the excitation period is smaller that $T_{\min}$, the system is not excitable thus cannot support traveling waves any more. One observes in Fig. 4 that $T_{\min}$ increases from top to bottom, suggesting the excitability in the top part of the system is larger than that in the bottom part. Although the diffusive coupling in the z direction may influence the wave propagation, the tendency of excitability distribution in the gradient direction should qualitatively coincide with that shown in Fig. 4. Thus, if the source period is smaller than the $T_{\min}$ of those middle and bottom layers, those layers could not support every wave emitted by the source. They can only support a more sparse wave train, like one of every two or more waves emitted from the source. This explains why some wave tails disappear in the middle of the system, resulting in an apparent wavelength or period multiplication in the projection image, as shown in the left part of Fig. 3(b).

When the spiral tip has a proper rotation period and a proper traveling speed, the Doppler effect may cause the effective period of wave source different beyond and behind the source movement. Together with the excitability difference explained above, this effect can cause the local wave grouping. In the instance of Fig. 3, the period (T_s) of the wave source at the spiral tip is 16.76 TU, and the drift speed (V_s) is 0.00424 SU/TU. According to the Doppler principle, the speeds and periods of forward and backward waves should satisfy the following equations:

$$T_- = \left(1 + \frac{V_s}{V_-}\right)T_s, \quad T_+ = \left(1 - \frac{V_s}{V_+}\right)T_s, \tag{2}$$

where V_- and V_+ are, respectively, the speeds of the waves behind and in front of the tip and T_- and T_+ are corresponding periods. Figure 5 gives the 2D crescent wave dispersion relation of the period T and speed V, where the curves $T_+(V_+)$ and $T_-(V_-)$ are calculated using Eqs. (2). The local periods T_- and T_+ are determined by the intersections of the curves. We see that in front of the tip, the period T_+ (reads 13.6 TU) is smaller than the low limit period ($T_{\min}$) of those middle and bottom layers (see Fig. 4), so that not every waves can extend to the middle and the bottom parts of the system. These parts of the system can support only double period $2T_+$ (27.2 TU) under the given conditions. As a result, the waves exhibit structures of grouping of every two waves. This explains wave grouping behavior observed in the experiments [Fig. 1(b)] and the simulations (Fig. 3). On the other hand behind the tip, the period of waves T_- (reads 19.6 TU) is large enough to be supported by almost all layers, and waves can hold good single periodicity.

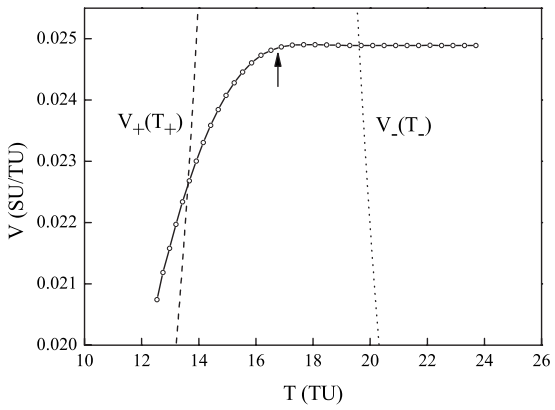

FIG. 5. Dispersion relation of the 2D crescent wave. The dashed and dotted lines are the velocity-period curves in front of and behind the tip of the spiral shown in Fig. 3(a), predicted by Eq. (2).

To explain how the wave grouping phenomenon appears and disappears as a function of control parameters, we scan the parameters space around the condition of Fig. 3. Every time we only change one parameter through the typical parameter set. Simulation indicates that with change of a parameter, the spiral state can experience a change from simply rotation to meandering and then to simply rotation. In the regime of meandering spiral, if the local period of the wave source is smaller than the maximal $T_{\min}$ in the system, wave grouping will take place. With some parameters, wavelength doubling can occur not only in meandering spirals but also in simply rotating spirals, which means waves "grouping" in all directions and thus line defects are inevitable. We thus suggest that line defects cannot only appear in a 2D reaction-diffusion system with a chaotic reaction kinetics as predicted in Refs. [23–26] and experimentally realized in Refs. [27–30], it can also happens in a 3D system with chemical gradients in one dimension. Here we use the control parameter A_l to demonstrate this effect. We compare the spiral period T and the maximal $T_{\min}$ among all layers as a function of A_l. The result is shown in Fig. 6. When A_l is low or high, spiral period T is always bigger than the maximal $T_{\min}$, so that the wave train is uniform in the system. Only in a small range of A_l $(0.03<A_l<0.06)T$ is smaller than the maximal $T_{\min}$. In these cases a portion of the system cannot support traveling waves, resulting in breaking up of the uniformity of the wave train and emerging of wave grouping patterns.

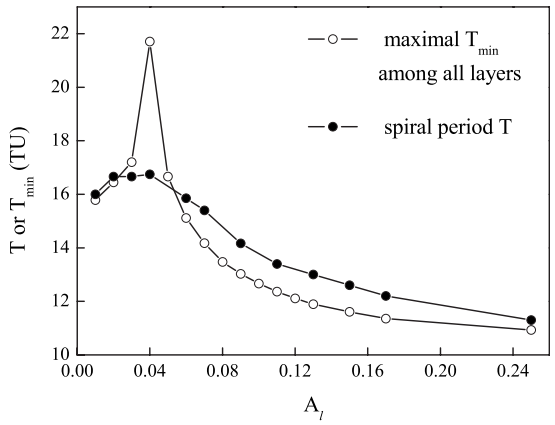

FIG. 6. The spiral period T and the maximal $T_{\min}$ among all layers at different A_l. Other parameters are the same as in Fig. 3.

IV. CONCLUSION

Comparing the results of experiments and simulations, we can deduct the following clues to explain the wave-grouping phenomena observed in the experiments: First, a meandering spiral with wave grouping can spontaneously occur in our 3D reaction-diffusion system. In contrast, in the corresponding 2D Oregonator system with oscillating dispersion, no spiral is found to meander. Second, wave grouping occurs from near the spiral tip, and waves in grouping have different shapes. These properties cannot be found in the aforementioned 2D system. In a 2D Oregonator system with oscillating dispersion, all excitable waves should have the same profile, and the spacings between the waves are just determined by the ripples of the recovery tail [27,31]. Thus even if waves emitted from the tip do not have the stable period, they can be excited temporarily with a similar unstable profile, providing the excitation period is bigger than the period of one exciting loop. In this case, the waves hold equal spacing for several periods until the unstable spacings slowly evolve to stable ones. In other words, the wave grouping process should have a convective nature, which is not observed in the experiments. Third, wave grouping goes in and out gradually with the change of some control parameters on the media surface. No bifurcation dynamics is identified during the process both in the experiments and in the simulations. This may reflect that the wave grouping is not a new phase, but a kind of coincidence of several factors. These factors include the leading spiral period T of the parameter gradient system, the distribution of the $T_{\min}$ among layers, and the meandering property of the spiral. With these arguments, we conclude that the 3D mechanism discussed in the above section is the reason for the formation of wave-grouping patterns observed in the experiments.

We also note some differences between the experiment and the simulation. In the experiment, the system will eventually enter into spiral turbulence when $[H_2SO_4]$ is high enough, however, the simulation based on the two-variable Oregonator model never demonstrates such spiral turbulence in our practice. It seems that the spiral in the simulation is much more stable than in the experiment. Another discordance is the influence of [MA] on the pattern formation. In the experiment, increasing [MA] can enhance the grouping phenomenon, but does not influence the wavelength. In the simulation, however, when B_u is high, spiral wavelength will increase remarkably, and waves will not group any more. Only lowering B_l will result in the more obvious wavelength doubling. These two discordancies might be caused by the simplification of the Oregonator model to the real ferroin-catalyzed BZ chemical reaction, and the unknown complicated relation between the stoichiometric coefficient f and A or B.

In conclusion, local wave grouping in our 3D BZ reaction system should be the projection of some oblique 3D wave structures caused by the reagent concentration gradients. The observed alternation of thick wave and thin wave is in fact the projection of long-tail wave and short-tail wave in the vertical direction of the reaction medium. Simulation based on the 3D hypothesis provides good proof for this mechanism. The observed difference of wave shape in the group in experiment can be well reproduced in simulation. We believe this work provide information to understand nonlinear waves in 3D reaction-diffusion systems.

ACKNOWLEDGMENT

This work was partially supported by the Chinese Natural Science Foundation and Minister of Science and Technology of China. Y.W. and J.Y. thank the support from the National Foundation for Fostering Talents of Basic Science (J0630311) and Jun-Zheng Foundation at Peking University.

[1] M. C. Cross and P. C. Hohenberg, Rev. Mod. Phys. **65**, 851 (1993).
[2] G. S. Skinner and H. L. Swinney, Physica D **48**, 1 (1991).
[3] I. Lengyel and I. R. Epstein, Science **251**, 650 (1991).
[4] T. Sakurai, E. Mihaliuk, F. Chirila, and K. Showalter, Science **296**, 2009 (2002).
[5] K. J. Lee, E. C. Cox, and R. E. Goldstein, Phys. Rev. Lett. **76**, 1174 (1996).
[6] E. L. Koschmieder and S. G. Pallas, Int. J. Heat Mass Transfer **17**, 991 (1974).
[7] Q. Ouyang and H. L. Swinney, Chaos **1**, 411 (1991).
[8] Q. Ouyang, H. L. Swinney, and G. Li, Phys. Rev. Lett. **84**, 1047 (2000).
[9] L.-Q. Zhou and Q. Ouyang, Phys. Rev. Lett. **85**, 1650 (2000).
[10] H.-M. Liao, L.-Q. Zhou, C.-X. Zhang, and Q. Ouyang, Phys. Rev. Lett. **95**, 238301 (2005).
[11] G. Li, Q. Ouyang, V. Petrov, and H. L. Swinney, Phys. Rev. Lett. **77**, 2105 (1996).
[12] V. Dufiet and J. Boissonade, Phys. Rev. E **53**, 4883 (1996).
[13] B. Sandstede and A. Scheel, Phys. Rev. Lett. **86**, 171 (2001).
[14] D. A. Vasquez, W. Horsthemke, and P. McCarty, J. Chem. Phys. **94**, 3829 (1991).
[15] J. P. Keener and J. J. Tyson, Physica D **21**, 307 (1986).
[16] W. Jahnke and A. T. Winfree, Int. J. Bifurcation Chaos Appl. Sci. Eng. **1**, 445 (1991).
[17] A. L. Belmonte, Q. Ouyang, and J.-M. Flesselles, J. Phys. II **7**, 1425 (1997).
[18] M. Dowle, R. M. Mantel, and D. Barkley, Int. J. Bifurcation Chaos Appl. Sci. Eng. **7**, 2529 (1997).
[19] Z. Noszticzius, W. Horsthemke, W. D. McCormick, H. L. Swinney, and W. Y. Tam, Nature (London) **329**, 619 (1987).
[20] N. Kreisberg, W. D. McCormick, and H. L. Swinney, J. Chem. Phys. **91**, 6532 (1989).
[21] E. Dulos, J. Boissonade, and P. De Kepper, in *Nonlinear Wave Processes in Excitable Media*, edited by A. V. Holden, M. Markus, and H. G. Othmer (Plenum, New York, 1991).
[22] E. Dulos, J. Boissonade, and P. De Kepper, Physica A **188**, 120 (1992).
[23] A. Goryachev, H. Chate, and R. Kapral, Phys. Rev. Lett. **80**, 873 (1998).
[24] A. Goryachev, H. Chate, and R. Kapral, Int. J. Bifurcation Chaos Appl. Sci. Eng. **9**, 2243 (1999).
[25] J. Davidsen, R. Erichsen, R. Kapral, and H. Chate, Phys. Rev. Lett. **93**, 018305 (2004).
[26] M. Zhan and R. Kapral, Phys. Rev. E **72**, 046221 (2005).
[27] K. J. Lee, Phys. Rev. Lett. **79**, 2907 (1997).
[28] J. S. Park and K. J. Lee, Phys. Rev. Lett. **83**, 5393 (1999).
[29] J. S. Park and K. J. Lee, Phys. Rev. Lett. **88**, 224501 (2002).
[30] J. S. Park, S. J. Woo, and K. J. Lee, Phys. Rev. Lett. **93**, 098302 (2004).
[31] J. Rinzel and K. Maginu, in *Nonequilibrium Dynamics in Chemical Systems*, edited by C. Vidal and A. Pacault (Springer, Berlin, 1984), p. 107.